

# Modular-DNA Programmed Molecular Construction of “Fixed” of 2D and 3D-Au Nanoparticle Arrays

Zhijie Ma, Wen Chen, Matthew C. Johnson, Ingeborg Schmidt-Krey, Loren Williams, and Gary B. Schuster\*

Georgia Institute of Technology, School of Chemistry and Biochemistry, Atlanta, Georgia 30332, United States

**S** Supporting Information

**ABSTRACT:** Specifically designed dimeric, planar trimeric, tetrameric, pentameric, and 3D hexameric assemblies of Au nanoparticles were constructed from self-assembling DNA modules that contain disulfide groups, for attachment to the nanoparticles, and covalently linked 2,5-bis(2-thienyl)pyrrole (SNS) monomers. Treatment of these arrays with horseradish peroxidase and H<sub>2</sub>O<sub>2</sub> (HRP/H<sub>2</sub>O<sub>2</sub>) results in bond formation between the SNS monomers that cross-links or ligates the DNA modules making the assemblies permanent (“fixed”).



## 1. INTRODUCTION

The programmable construction of precisely ordered complex metal nanoparticle arrays is expected to provide advanced materials having unique structures and properties.<sup>1–3</sup> Over the past 20 years, various methods employing nucleic acids, peptides and proteins, microorganisms, and physical templates have been used to prepare nanoparticles arrays.<sup>4</sup> Among these options, nucleic acids are currently the most promising candidate for their general, programmed assembly.<sup>5</sup> Building upon the pioneering work of Mirkin<sup>6</sup> and Alivisatos,<sup>7</sup> a diverse set of metal nanoparticle arrays have been constructed using the self-recognizing properties of DNA to direct the formation of these materials.<sup>8–23</sup> Recently, DNA origami has been applied to the assembly of metal nanoparticle arrays enabling the formation of precise, relatively stiff structures.<sup>24–27</sup> DNA programmed nanoparticle arrays have found application in, for example, the construction of plasmonic absorbers,<sup>28–33</sup> and they may be useful as optical cloaking materials.<sup>34,35</sup>

Despite successes in the construction of metal nanoparticles arrays using nucleic acids, there are still significant obstacles to overcome. Remaining challenges that have been identified include the ability to design and construct complicated and controlled multifunctional structures that incorporate diverse components having specific functions.<sup>36</sup> And, significantly, because of the reversibility of Watson–Crick hydrogen bonding, arrays constructed with nucleic acids scaffolds are not permanent. DNA duplexes typically denature in water solution without added salt and at elevated temperature.<sup>37</sup> Several approaches to make permanent or “fix” DNA arrays have recently been reported. Photo-cross-linking<sup>38–40</sup> and “click” chemistry<sup>41</sup> procedures form covalent bonds between two DNA strands making them inseparable, and encapsulation<sup>42</sup> enables the use of DNA-containing nanoparticle arrays in the solid-state. Furthermore, in current applications, DNA plays an exclusively structural role as a scaffold in the assembly of

metal nanoparticle arrays. The nanoparticles in these arrays interact exclusively through space and not through the structural components that enabled their assembly.

We are developing conjoined DNA-conducting polymer systems as a means to fix DNA assemblies, incorporate sequence information of the DNA into the conjoined polymer and to confer the electronic properties of the conducting polymer on the DNA scaffold.<sup>43–49</sup> In this approach, monomers of conducting polymers, 2,5-bis(2-thienyl)pyrrole (SNS), for example (see Scheme 1), are linked covalently to nucleic acid bases of DNA oligomers. The oxidative polymerization of these monomers with horseradish peroxidase and hydrogen peroxide (HRP/H<sub>2</sub>O<sub>2</sub>) forms conducting polymers of controlled length and composition that can cross-link or ligate DNA oligomers. In this article, we describe the programmed preparation of two and three-dimensional arrays of Au nanoparticles constructed from self-recognizing DNA modules containing covalently linked cyclic disulfides<sup>50,51</sup> and SNS monomers. The arrays are assembled by hybridization of DNA modules, attached to a Au nanoparticle (through the disulfide group), and the DNA scaffold is fixed by reaction of the SNS monomers to form a polymer that cross-links or ligates the modules, see Scheme 1. These arrays may be especially useful in applications where assemblies formed from unmodified DNA would denature.

## 2. EXPERIMENTAL SECTION

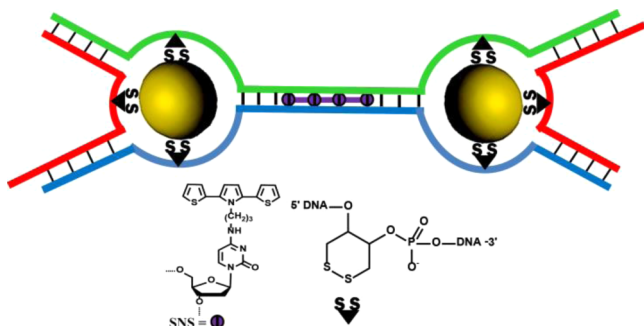
**2.1. Materials.** All commercially available reagents were used without further purification. Au nanoparticles of 5 and 10 nm diameter were purchased from Ted Pella or prepared according to the reported method.<sup>52,53</sup> Bis(p-sulfonatophenyl) phenylphosphine dehydrate

Received: April 22, 2014

Revised: September 9, 2014

Published: September 15, 2014

**Scheme 1. Representation of a Fixed Au Nanoparticle Dimer Assembled from Three DNA modules and “Fixed” By Crosslinking with a Conjoined SNS Polymer<sup>a</sup>**



<sup>a</sup>The green, red, and blue colored lines represent the DNA strands of each module (see Figure 2 for the actual DNA structures) that are partially complementary and form double stranded “arms” in the regions shown as connected by black bars. The connected purple spheres represent SNS monomers that have been linked by reaction with HRP/H<sub>2</sub>O<sub>2</sub>. Each module contains a disulfide groups (SS) that binds to the Au nanoparticles (the gold colored spheres) in the array.

dipotassium salt was purchased from Sigma-Aldrich. Centrifugal filter units with membrane Ultracel low binding regenerated cellulose were purchased from Millipore. Dithiol phosphoramidite was purchased from Glen Research. SNS containing modified DNA oligomers were synthesized as previously reported.<sup>45</sup> Horseradish peroxidase (HRP), type II (200 units/mg) and 2,2'-azino-bis(3-ethylbenzothiazoline-6-sulfonic acid) (ABTS) were purchased from Sigma-Aldrich, St. Louis, MO. A stock solution of HRP was prepared by dissolving 2 mg of HRP in 1 mL of nanopure water. Hydrogen peroxide was purchased from Fischer Scientific, Pittsburgh, PA, and diluted with Dnase free water to 0.03% before use.

**2.1.1. Au Nanoparticles Complexation and Concentration.** Au nanoparticles were capped with bis(p-sulfonatophenyl) phenylphosphine according to the described method<sup>8</sup> and concentrated by centrifugation with centrifugal filter units to 5–10  $\mu$ M for 5 nm and 0.5–1.0  $\mu$ M for 10 nm particles as a stock solution.

**2.1.2. Purification of Modified DNA Oligomers.** The DNA oligomers were purified by reverse phase HPLC using a Dynamax C18 column. The purified DNA was desalted with Waters Sep Pak cartridge and characterized by ESI-mass spectrometry. The concentration of the SNS-modified DNA was measured by its absorption intensity at 260 nm with every two SNS groups counted as one cytosine.

**2.1.3.  $T_m$  Measurements.** Samples were prepared by hybridization of 1  $\mu$ M solutions of DNA oligomers in 10 mM of sodium citrate buffer (pH 4.5, where HRP activity is maintained) with 200 mM of NaCl. The melting curves were measured at heating and cooling rates of 1  $^{\circ}$ C/min.  $T_m$  values were determined by differentiation of melting curves. UV-vis spectra were recorded on a Cary 1E spectrophotometer.

**2.1.4. Ligation of SNS-Modified DNA Duplexes.** Samples were prepared by hybridizing 0.5–2  $\mu$ M solutions of the desired single-strand DNA oligomers in 10 mM citrate buffer (pH 4.5) containing 200 mM of NaCl. Hybridization was achieved by heating the samples at 80  $^{\circ}$ C for 10 min then cooling to 15  $^{\circ}$ C at a rate of 1  $^{\circ}$ C/min. The ligation reaction was performed at 15  $^{\circ}$ C in 1 mL of solution by addition of 5  $\mu$ L of HRP (2 mg dissolved in 1 mL of nanopure water) followed by 2  $\mu$ L of H<sub>2</sub>O<sub>2</sub> (0.03%) and 2  $\mu$ L of ABTS (20  $\mu$ M in water). UV-vis spectra were recorded before and after initiation of reaction.

**2.2. Nanoparticle Assembly.** **2.2.1. Au-DNA(1,2) Dimer, Au-DNA(6,7,8) Trimer, Au-DNA(6,7,9,10) Tetramer, Au-DNA(6,7,9,11,12) Pentamer, and Au-DNA(13,14,15) Hexamer.** Samples were prepared by mixing 30  $\mu$ L of a 1.66  $\mu$ M solution of 5 nm Au nanoparticles or 30  $\mu$ L of a 0.166  $\mu$ M solution of 10 nm or 13 nm

nanoparticles with different ratios of cross-linked DNA(1,2), DNA-(6,7,8), DNA(6,7,9,10), DNA(6,7,9,11,12), or DNA(13,14,15) in 10 mM sodium phosphate (pH = 7.0), 50–100 mM sodium chloride solution and hybridizing overnight.

**2.2.2. Au-DNA(3,4,5) Dimer.** Samples of 5 and 10 nm Au nanoparticles having a single attached strand of DNA(3) were synthesized and purified with T85, a long DNA for the purification according to the reported procedure.<sup>15,29</sup> Samples were prepared by heating the cross-linked DNA(4,5) solutions at 80  $^{\circ}$ C for 2 min and then annealing with 5 or 10 nm DNA(3)/T85Au nanoparticles with appropriate ratios of cross-linked DNA(4,5) in 10 mM sodium phosphate (pH = 7.0), 100 mM sodium chloride solution overnight.

**2.2.3. Nanoparticle Assembly Purification.** An agarose gel (2–3%) was used to purify the Au nanoparticle assemblies and tris-borate EDTA (0.5 $\times$ , TBE) was used as running buffer. Before loading, the samples were mixed with 10  $\mu$ L of 0.5 $\times$  TEB and 4  $\mu$ L of 50% Ficoll 400. A voltage of 50 V was used for the electrophoresis. After electrophoresis, the desired bands were sliced and put into dialysis membranes mixed with 4–5 mL of water. The Au nanoparticle assemblies were separated by gel electrophoresis. Then 5 M of ammonium acetate or sodium chloride solution was added to adjust the salt concentration to 50–100 mM. The solution was concentrated by centrifugation with centrifugal filter units. For samples in water, the buffer solution was removed by washing 100  $\mu$ L samples with 1–2 mL of nanopure water and centrifuging with centrifugal filter units. This process was repeated at least three times to ensure that the buffer was completely removed.

**2.2.4. TEM Procedures.** A JEOL TEM 100CX was used to characterize the Au nanoparticle assemblies. A copper grid with carbon film on 150 meshes was used. Typically, a 10  $\mu$ L solution of Au nanoparticle assemblies was dropped on the grid and deposited for 1–2 min. Excess solution was removed and the grid was dried in air for 1 h.

**2.2.5. Cryo EM Procedures.** A JEOL JEM-1400 and a Gatan 626 holder were used for the cryo-EM studies. Samples were prepared by the “back injection” technique.<sup>54</sup> Briefly, a small piece of carbon film was floated on a droplet of 4% trehalose solution and picked up with a clean EM grid. The grid was then inverted and 1.5  $\mu$ L of sample was pipetted into the buffer droplet on the “back” of the grid. After a 60 s incubation period, the grid was blotted, air-dried for 10 s, and rapidly plunged into liquid nitrogen resulting in a thin layer of vitreous ice.

**2.2.6. Optical Spectra of the 10 nm Au Trimer.** A 0.1 mL UV cuvette was used for measurement of the optical spectrum of Au nanoparticles and Au trimer assemblies. UV-vis spectra were recorded at room temperature on a Cary 1E spectrophotometer.

### 3. RESULTS AND DISCUSSION

**3.1. Au Dimers.** The simplest structure prepared by the encoded module approach is comprised of two Au nanoparticles connected by a cross-linked DNA duplex to form a “dumbbell” shaped assembly, see Figure 1. This nanoparticle dimer was prepared from two complementary oligonucleotides, DNA(1) and (2), synthesized according to standard procedures, both of which are modified to contain the cyclic disulfide group (SS) at their 3'-termini and each containing two covalently linked SNS monomers (X) arranged so that they are aligned at adjacent sites in the major groove of the duplex.<sup>49</sup> The two DNA strands were hybridized and treated with HRP/H<sub>2</sub>O<sub>2</sub> resulting in their cross-linking, which was confirmed by the increase in  $T_m$  from 61 to 72  $^{\circ}$ C and by optical spectroscopy of the conducting polymer (see Figure S1 in the Supporting Information).<sup>49,55</sup> The cross-linked duplex was mixed with 5 or 10 nm diameter phosphine-capped Au nanoparticles,<sup>8</sup> and the resulting assembly was purified by agarose gel electrophoresis using standard techniques giving dimers in  $\sim$ 82% purity (see Figures S2–S4 and Table S2 in the Supporting Information).<sup>56</sup>

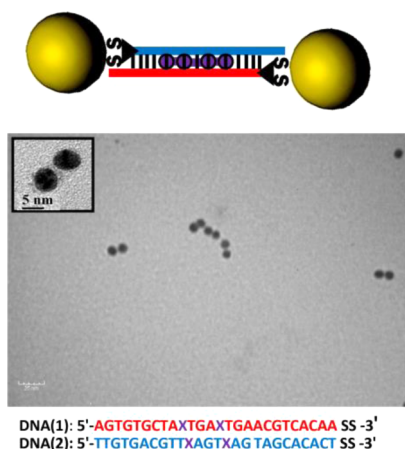


**Figure 1.** Au nanoparticle dimer in water (where the symbols have the same meaning as in Scheme 1) shown schematically above the TEM image of the array. The actual DNA sequences are shown below the TEM image where “X” represents the SNS-linked cytosine nucleotides. The inset is a cryoelectron microscopy image of a similar 5 nm Au nanoparticle dimer.

A TEM image of the dumbbell array was recorded on a 150 mesh copper grid revealing dimers that remain intact when dispersed in water, see Figure 1. Control experiments (see Figure S5 in the Supporting Information) show that similar non-cross-linked Au nanoparticle arrays disintegrate in water. Interestingly, the interparticle distance revealed in Figure 1 and Table S1 in the Supporting Information is 3.6 nm, less than the ~8.5 nm predicted for a fully extended duplex DNA scaffold, which suggests that the assembly might be bent. The inset in Figure 1 shows a cryoelectron microscopy image of a similar assembly prepared from 5 nm Au particles where the interparticle distance is measured to be 2.5 nm. The development of more elaborate cross-linked DNA scaffolds gives arrays having readily predictable nanoparticle arrangements and distances.

The two particle array shown in Scheme 1 is comprised of three DNA modules whose structures are shown as DNA(3,4,5) in Figure 2. DNA(3) contains a single disulfide group for attachment to a Au nanoparticle and contains recognition sequences on both its 3'- and 5'-ends that are complementary

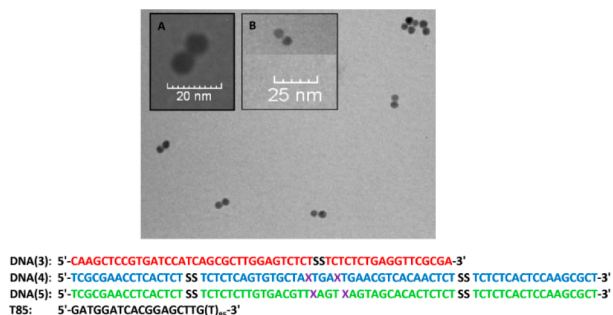


**Figure 2.** TEM image of a Au nanoparticle dimer array in water assembled from three DNA modules and cross-linked by reaction of the SNS monomers with HRP/H<sub>2</sub>O<sub>2</sub>, as represented in Scheme 1. The DNA sequences are shown below the TEM image where “X” represents the SNS-linked cytosine nucleotides and SS stands for the disulfide group. Inset A shows an expanded view of the dimers prepared from 10 nm Au particles; inset B shows the related assembly prepared from 5 nm Au particles.

to corresponding sequences in DNA(4) and DNA(5). DNA(3) also contains a “target” sequence that is complementary to the T85 oligomer used as an auxiliary in the agarose gel purification of the DNA-linked Au nanoparticles.<sup>56</sup> The DNA(4) and (5) modules each contain two disulfide groups and two SNS monomers arranged, as indicated in Scheme 1, so that each module is linked to a Au nanoparticle and the SNS monomers are aligned in the major groove of the common “arm” that connects the two nanoparticles. This two particle array was assembled in three steps. First, DNA(3) was linked to a 5 or 10 nm Au nanoparticle and purified by agarose gel electrophoresis with, T85, a long DNA oligomer assisting the purification as reported (see Figure S6 in the Supporting Information).<sup>15,29</sup> Second, DNA(4) and DNA(5) were hybridized and then treated with HRP/H<sub>2</sub>O<sub>2</sub>. Formation of the cross-linked two-module assembly from DNA(4) and (5) was confirmed by an increase in  $T_m$  from 56 to 73 °C and by optical spectroscopy, which shows the appearance of polaron bands typical of conducting polymers (see Figure S7 in the Supporting Information). Finally, Au-linked DNA(3) and the cross-linked two-module assembly were annealed in buffer solution by heating to 80 °C for 2 min and then slow cooling overnight. The two particle arrays, isolated by agarose gel (see Figure S8 in the Supporting Information) in ~85% purity (see Table S2 in the Supporting Information) and dispersed in water, were analyzed by TEM, see Figure 2. While the distance between the 5 nm–5 nm Au nanoparticles in the dimers is 2.5 nm, which is significantly less than the corresponding calculated distance of 7.4 nm (see Table S2 in the Supporting Information) possibly due to the flexibility of the DNA, the distance between the 10 nm–10 nm Au nanoparticles in the dimers is 0.9 nm, which is somewhat less than the corresponding calculated distances of 2.4 nm (see Table S2 in the Supporting Information). These assemblies are fixed; they do not dissociate when dispersed in water (see Figure 2, Figure S9 in the Supporting Information). Control experiments (see Figure S10 in the Supporting Information) show that similar non-cross-linked Au nanoparticle arrays disintegrate in water.

**3.2. Planar Au Trimers, Tetramers, and Pentamers.** A related modular DNA self-assembly strategy was used to prepare multiparticle Au arrays, see Figure 3. The three-module DNA(6,7,8) cyclic scaffold was first formed by self-assembly and then ligated by reaction with HRP/H<sub>2</sub>O<sub>2</sub>. Formation of the ligated assembly was confirmed by the observed increase in  $T_m$  from 70 to 83 °C and by characteristic changes to the optical spectrum (see Figure S11 in the Supporting Information).<sup>46</sup> The cross-linked assembly was mixed with 5 nm diameter phosphine-capped Au nanoparticles,<sup>8</sup> and the resulting three Au nanoparticle array was purified by agarose gel electrophoresis using standard techniques and isolated in ~71% purity (see Table S2 and Figures S12–S14 in the Supporting Information).<sup>56</sup> Shown in Figure 3 is the TEM image of the Au nanoparticle trimer dispersed in water formed by self-assembly and ligation of the DNA modules. A similar modular DNA self-assembly strategy was also used to prepare tetrameric and pentameric Au nanoparticle arrays, see Figure 4. The four-module DNA(6,7,9,10) cyclic scaffold and five-module DNA(6,7,9,11,12) cyclic scaffolds were formed by self-assembly and then ligated by reaction with HRP/H<sub>2</sub>O<sub>2</sub>. Formation of the ligated cyclic assemblies DNA(6,7,9,10) DNA(6,7,9,11,12) were confirmed by the observed increase in  $T_m$  from 60 to 80 °C and from 59 to 80 °C and by characteristic changes to the optical spectrum, respectively (see Figures S16 and S17 in

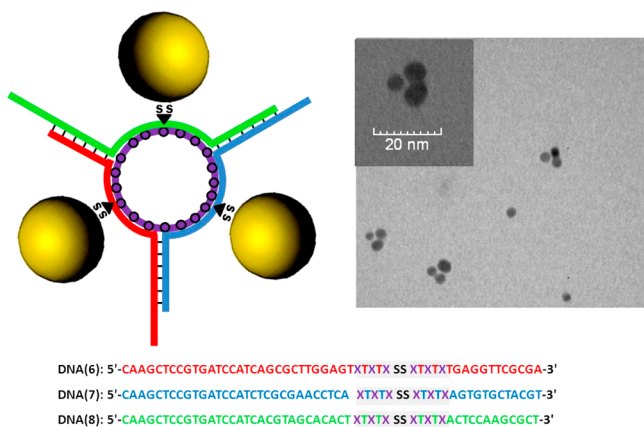


**Figure 3.** Schematic representation of the Au nanoparticle trimer formed by self-assembly of three DNA modules (the symbols have the same meaning as in Scheme 1) and the TEM image of 5 nm Au nanoparticle array in water ligated by reaction of the SNS monomers with HRP/H<sub>2</sub>O<sub>2</sub>. The DNA sequences are shown where “X” represents the SNS-linked cytosine nucleotides and SS stands for the disulfide group; the “grayed” regions in the sequences correspond to the single-stranded portion of the cyclic array.

the Supporting Information). Similarly, purified planar tetrameric and pentameric Au particle arrays were constructed by treating Au nanoparticles with the cross-linked four-module DNA(6,7,9,10) and five-module DNA(6,7,9,11,12) scaffolds. TEM images are shown in Figure 4 of the Au nanoparticle tetrameric and pentameric arrays that have been dispersed in water (see Figures S18, S19, and S21 in the Supporting Information). The purities of the Au tetrameric and pentameric arrays are 51% and 48%, respectively (see Table S2 in the Supporting Information). The distances between the Au trimeric, tetrameric, and pentameric arrays are measured to be 2.2, 2.9, and 3.1 nm (see Table S2 in the Supporting Information), which are slightly less than the corresponding calculated distance of 3.1, 3.4, and 3.5 nm assuming a circular shape for the conjoined poly(SNS)/DNA scaffold. The control experiments (see Figures S15, S20, and S22 in the Supporting Information) show that similar non-cross-linked Au trimer, tetramer, and pentamer nanoparticle arrays disintegrate in water.

**3.3. Three-Dimensional Hexameric Assemblies.** The construction of DNA-based objects has progressed from simple two-dimensional shapes to more complex three-dimensional constructs.<sup>3,19,57</sup> One of the most elegant of these structures was constructed by Seeman and used to build an engineered crystal based upon DNA oligomers fashioned into a tensegrity triangle.<sup>58</sup> We built on this work by extending the length of the DNA oligomers that form the triangle and by incorporating SNS monomers enabling cross-linking that fixes the structure and, finally, included disulfide groups used to bind Au nanoparticles. This spontaneously assembling structure was used to prepare permanent 3D hexameric Au nanoparticle arrays with predictable orientation and dimensions.

The seven-module scaffold containing three DNA strands DNA(13,14,15) in a ratio 3:3:1 was designed to assemble into a 3D structure so that each module contains two covalently linked SNS monomers (X) that are aligned at adjacent sites in the major groove and are flanked by seven base pairs at both ends to stabilize the structure. DNA(13) and DNA(14) contain the cyclic disulfide group (SS) at their 3'-termini, which was protected from hydrolysis by an extending thymine, see Figure 5. The 3D structure was formed by self-assembly and then cross-linked by coupling of adjacent SNS monomers with HRP/H<sub>2</sub>O<sub>2</sub>. Formation of the ligated assembly was confirmed by the increase in *T<sub>m</sub>* from 47 to 61 °C and by characteristic changes of the optical spectrum (see Figure S23 in the Supporting Information). Agarose gel electrophoresis confirmed the formation of the assembly which remains intact after the solution is desalted (see Figure S24 in the Supporting Information). The cross-linked assembly was mixed with phosphine-capped 5 or 10 nm Au nanoparticles and the resulting six Au nanoparticle array was purified by agarose gel electrophoresis (see Figures S25–27 in the Supporting Information) using standard techniques. The structure containing six Au nanoparticles was isolated in ~49% purity (see Table S2 in the Supporting Information). The distance between the Au hexameric arrays is measured to be 2.7 nm (see Table S2 in the Supporting Information), which is in agreement with the calculated distance of 2.9 nm. The control experiments (see Figure S28 in the Supporting Information) show that similar non-cross-linked Au hexameric nanoparticle arrays disintegrate in water.

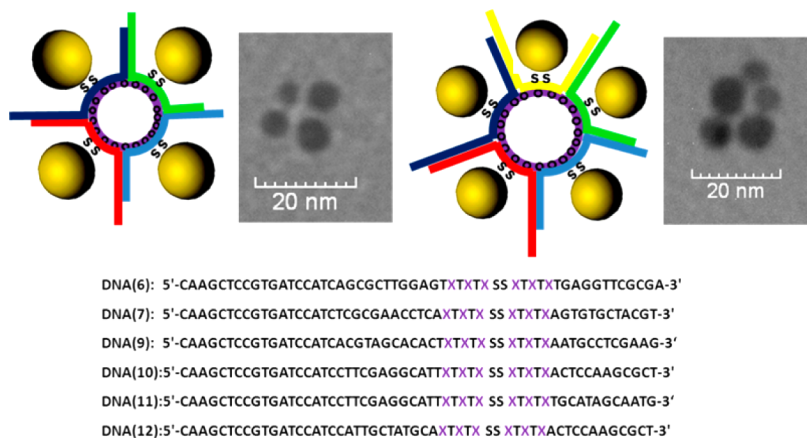
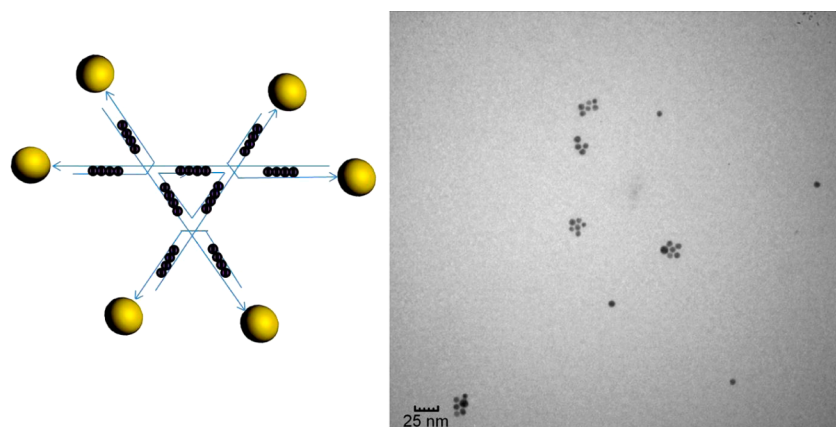


**Figure 4.** Schematic representation of the Au nanoparticle tetramer and pentamer formed by self-assembly of four DNA modules (the symbols have the same meaning as in Figure 3) and the TEM image of 5 nm Au nanoparticle array in water ligated by reaction of the SNS monomers with HRP/H<sub>2</sub>O<sub>2</sub>.



DNA(13): 5'-ACTATTGAGTXAGTXTCGGACAGGCATCAAGTXAGTXAGTATGTCGGACGAAGTXAGTXATCTACGAGSSST-3'

DNA(14): 5'-CGTAGATGAXTGAXTTCGTCGGTGTCCGGAGXTGAXTCAATAGTCTSSST-3'

DNA(15): 5'-GAXTTGATGCCACATACTGAXTGAXTTGATGCCACATACTGAXTGAXTTGATGCCACATACTGAXT-3'

**Figure 5.** Schematic representation of the Au nanoparticle hexamer formed by self-assembly of three DNA modules and the TEM image of 5 nm Au nanoparticle array in water ligated by reaction of the SNS monomers with HRP/H<sub>2</sub>O<sub>2</sub>. The DNA sequences are shown where “X” represents the SNS-linked cytosine nucleotides and SS stands for the disulfide group. The purple spheres represent the polymerized SNS monomers.

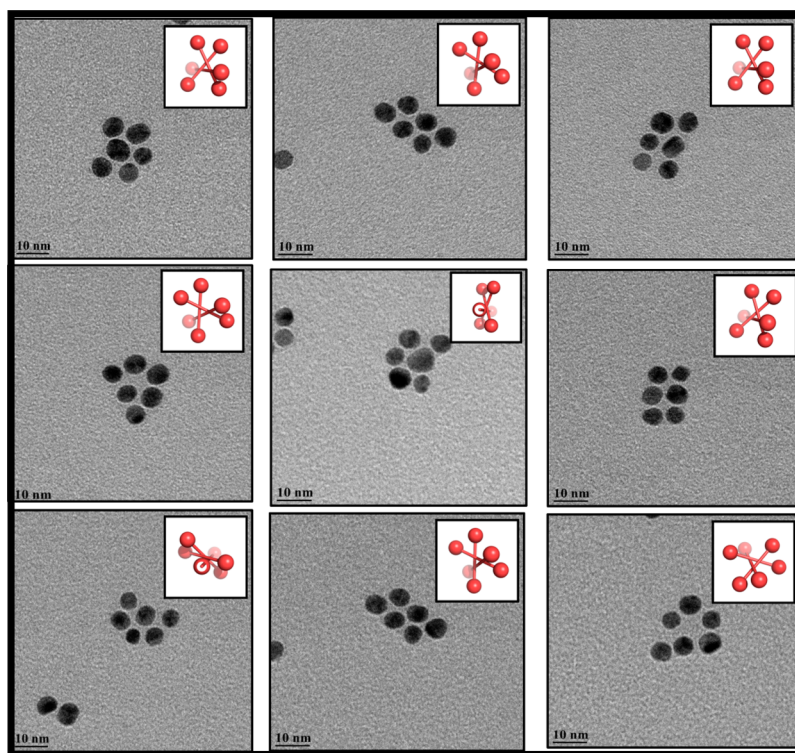


**Figure 6.** Cryo-TEM image of 5 nm Au nanoparticle hexamer array ligated by reaction of the SNS monomers with HRP/H<sub>2</sub>O<sub>2</sub>. The insets show models of the hexameric array formed into 3D arrays assuming that the DNA is in its standard B-form. The model structures are oriented in 3D space so that the position of the Au nanoparticles corresponds with that of those in the 2D cryo-TEM image.

The structure of the expected 3D array was modeled by assuming the standard B-DNA structure having a rise of 3.4 Å per base pair and 10 base pairs per 360° helical turn. This model is shown in comparison with cryoelectron microscopy images of the assemblies in Figure 6. A tomographic movie from the cryoelectron microscopy images is included in the Supporting Information. Clearly, the expected assembly is formed and the SNS linkages fix the structure so that it is permanent.

**3.4. Optical Absorption.** The optical absorption spectra of the 10 nm Au nanoparticles and those of their trimeric assemblies are shown in Figure 7. Within the resolution of the measurement, the absorption maximum of the surface plasmon resonance band is unaffected by assembly into the trimer and by its cross-linking.<sup>59</sup> However, it appears that formation of the trimer and its cross-linking by reaction of their SNS monomers with HRP/H<sub>2</sub>O<sub>2</sub> results in broadening due to plasmon enhanced scattering.<sup>33</sup> This suggests that after the cross-linking reaction the Au particles have become closer or that the

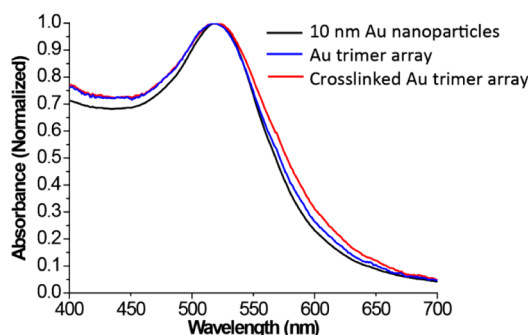


**Figure 7.** Absorption spectra of Au nanoparticle arrays normalized to the same absorbance value. There is no measurable shift in the absorption maximum compared with single particles (black line). The spectrum of the trimer array (blue line) is broader than that of the single particle, and the spectrum of the ligated trimer array (red line) is broadened further.

conducting polymer interacts electronically with the nanoparticle.

A calculated spectrum of the trimeric arrays for 5 and 10 nm particles at an assigned separation distance of 3 nm is shown in Figure S29 in the Supporting Information. The calculated average spectrum for the 10 nm particles has an apparent maximum at 524 nm, which is similar to that of the observed spectrum which exhibits a maximum at  $520 \pm 1$  nm. The calculated spectrum of the array is shifted 3.5 nm to the red and broadened compared with the unassembled Au particle. Similar effects have been previously reported and attributed to increased scattering.<sup>33</sup> Experimentally, we observe only broadening, which is consistent with the previous report for small particles.<sup>33</sup>

#### 4. CONCLUSIONS

In summary, we have shown that robust, fixed Au nanoparticle arrays can be easily assembled from DNA modules that contain three functional units: (i) recognition sequences that guide assembly according to Watson–Crick base pairing rules; (ii) appropriately positioned SNS monomers whose reaction with HRP/H<sub>2</sub>O<sub>2</sub> will cross-link or ligate the DNA modules so that they become inseparable; (iii) disulfide groups placed within the DNA module to bind and hold a Au nanoparticle. The arrays we describe are comprised of two, three, four, five, and six Au nanoparticles, and it is clear that this approach can enable the construction of more complex structures. The conducting polymers used to fix these arrays appear to play an exclusively structural role in the arrays reported here. However, this approach may be extended so that the electronic properties of the conducting polymer can be incorporated into the functional characteristics of metal nanoparticle arrays.

#### ■ ASSOCIATED CONTENT

##### Supporting Information

Mass analysis of the DNA oligomers, UV spectrum and melting curves of the DNA assemblies, and agarose gel and TEM images of Au nanoparticle assemblies. This material is available free of charge via the Internet at <http://pubs.acs.org>.

#### ■ AUTHOR INFORMATION

##### Corresponding Author

\*E-mail: [schuster@gatech.edu](mailto:schuster@gatech.edu).

#### Notes

The authors declare no competing financial interest.

#### ■ ACKNOWLEDGMENTS

This work was supported by the Vasser Woolley Foundation, for which we are grateful. The TEM images were recorded at the Georgia Tech Center for Nanostructure Characterization. We thank Professor Mostafa El-Sayed and Ms. Rachel Near for assistance in calculation of the optical spectrum.

#### ■ REFERENCES

- (1) Toffoli, T.; Margolus, N. *Phys. D* **1991**, *47*, 263–272.
- (2) Winfree, E.; Liu, F. R.; Wenzler, L. A.; Seeman, N. C. *Nature* **1998**, *394*, 539–544.
- (3) Kim, J. W.; Kim, J. H.; Deaton, R. *Angew. Chem., Int. Ed.* **2011**, *50*, 9185–9190.
- (4) Jones, M. R.; Osberg, K. D.; Macfarlane, R. J.; Langille, M. R.; Mirkin, C. A. *Chem. Rev.* **2011**, *111*, 3736–3827.
- (5) Tan, S. J.; Campolongo, M. J.; Luo, D.; Cheng, W. L. *Nat. Nanotechnol.* **2011**, *6*, 268–276.
- (6) Mirkin, C. A.; Letsinger, R. L.; Mucic, R. C.; Storhoff, J. J. *Nature* **1996**, *382*, 607–609.
- (7) Alivisatos, A. P.; Johnsson, K. P.; Peng, X. G.; Wilson, T. E.; Loweth, C. J.; Bruchez, M. P.; Schultz, P. G. *Nature* **1996**, *382*, 609–611.
- (8) Loweth, C. J.; Caldwell, W. B.; Peng, X. G.; Alivisatos, A. P.; Schultz, P. G. *Angew. Chem., Int. Ed.* **1999**, *38*, 1808–1812.
- (9) Zanchet, D.; Micheel, C. M.; Parak, W. J.; Gerion, D.; Williams, S. C.; Alivisatos, A. P. *J. Phys. Chem. B* **2002**, *106*, 11758–11763.
- (10) Wang, G. L.; Murray, R. W. *Nano Lett.* **2004**, *4*, 95–101.
- (11) Le, J. D.; Pinto, Y.; Seeman, N. C.; Musier-Forsyth, K.; Taton, T. A.; Kiehl, R. A. *Nano Lett.* **2004**, *4*, 2343–2347.
- (12) Deng, Z. X.; Tian, Y.; Lee, S. H.; Ribbe, A. E.; Mao, C. D. *Angew. Chem., Int. Ed.* **2005**, *44*, 3582–3585.
- (13) Xu, X. Y.; Rosi, N. L.; Wang, Y. H.; Huo, F. W.; Mirkin, C. A. *J. Am. Chem. Soc.* **2006**, *128*, 9286–9287.
- (14) Zheng, J. W.; Constantinou, P. E.; Micheel, C.; Alivisatos, A. P.; Kiehl, R. A.; Seeman, N. C. *Nano Lett.* **2006**, *6*, 1502–1504.
- (15) Aldaye, F. A.; Sleiman, H. F. *J. Am. Chem. Soc.* **2007**, *129*, 4130–4131.
- (16) Nykypanchuk, D.; Maye, M. M.; van der Lelie, D.; Gang, O. *Nature* **2008**, *451*, 549–552.
- (17) Park, S. Y.; Lytton-Jean, A. K. R.; Lee, B.; Weigand, S.; Schatz, G. C.; Mirkin, C. A. *Nature* **2008**, *451*, 553–556.
- (18) Sharma, J.; Chhabra, R.; Cheng, A.; Brownell, J.; Liu, Y.; Yan, H. *Science* **2009**, *323*, 112–116.
- (19) Mastroianni, A. J.; Claridge, S. A.; Alivisatos, A. P. *J. Am. Chem. Soc.* **2009**, *131*, 8455–8459.
- (20) Maye, M. M.; Nykypanchuk, D.; Cuisinier, M.; van der Lelie, D.; Gang, O. *Nat. Mater.* **2009**, *8*, 388–391.
- (21) Lo, P. K.; Karam, P.; Aldaye, F. A.; McLaughlin, C. K.; Hamblin, G. D.; Cosa, G.; Sleiman, H. F. *Nat. Chem.* **2010**, *2*, 319–328.
- (22) Wu, J. Y.; Silvent, J.; Coradin, T.; Aime, C. *Langmuir* **2012**, *28*, 2156–2165.
- (23) Wilner, O. I.; Willner, I. *Chem. Rev.* **2012**, *112*, 2528–2556.
- (24) Pal, S.; Deng, Z. T.; Ding, B. Q.; Yan, H.; Liu, Y. *Angew. Chem., Int. Ed.* **2010**, *49*, 2700–2704.
- (25) Ding, B. Q.; Deng, Z. T.; Yan, H.; Cabrini, S.; Zuckermann, R. N.; Bokor, J. *J. Am. Chem. Soc.* **2010**, *132*, 3248–3249.
- (26) Hung, A. M.; Micheel, C. M.; Bozano, L. D.; Osterbur, L. W.; Wallraff, G. M.; Cha, J. N. *Nat. Nanotechnol.* **2010**, *5*, 121–126.
- (27) Stulz, E. *Chem.—Eur. J.* **2012**, *18*, 4456–4469.
- (28) Fan, J. A.; He, Y.; Bao, K.; Wu, C. H.; Bao, J. M.; Schade, N. B.; Manoharan, V. N.; Shvets, G.; Nordlander, P.; Liu, D. R.; Capasso, F. *Nano Lett.* **2011**, *11*, 4859–4864.
- (29) Busson, M. P.; Rolly, B.; Stout, B.; Bonod, N.; Larquet, E.; Polman, A.; Bidault, S. *Nano Lett.* **2011**, *11*, 5060–5065.

- (30) Halas, N. J.; Lal, S.; Chang, W. S.; Link, S.; Nordlander, P. *Chem. Rev.* **2011**, *111*, 3913–3961.
- (31) Chen, Y.; Cheng, W. L. *Wiley Interdiscip. Rev.: Nanomed. Nanobiotechnol.* **2012**, *4*, 587–604.
- (32) Watanabe-Tamaki, R.; Ishikawa, A.; Tanaka, T.; Zako, T.; Maeda, M. *J. Phys. Chem. C* **2012**, *116*, 15028–15033.
- (33) Lan, X.; Chen, Z.; Liu, B. J.; Ren, B.; Henzie, J.; Wang, Q. B. *Small* **2013**, *9*, 2308–2315.
- (34) Ishikawa, A.; Tanaka, T.; Kawata, S. *Phys. Rev. Lett.* **2005**, *95*, 237401.
- (35) Ishikawa, A.; Tanaka, T.; Kawata, S. *J. Opt. Soc. Am. B: Opt. Phys.* **2007**, *24*, 510–515.
- (36) Lee, J. S.; Song, J. J.; Deaton, R.; Kim, J. W. *Biomed. Res. Int.* **2013**, *2013*, No. 310461.
- (37) Horton, H. R.; Moran, L. A.; Ochs, R. S.; Rawn, J. D.; Scrimgeour, K. G. *Principles of Biochemistry*, 2nd ed.; Prentice Hall: Upper Saddle River, NJ, 1996.
- (38) Ogasawara, S.; Fujimoto, K. *ChemBioChem* **2005**, *6*, 1756–1760.
- (39) Ohshiro, T.; Zako, T.; Watanabe-Tamaki, R.; Tanaka, T.; Maeda, M. *Chem. Commun.* **2010**, *46*, 6132–6134.
- (40) Gerrard, S. R.; Hardiman, C.; Shelbourne, M.; Nandhakumar, I.; Norden, B.; Brown, T. *ACS Nano* **2012**, *6*, 9221–9228.
- (41) Lundberg, E. P.; El-Sagheer, A. H.; Kocalka, P.; Wilhelmsson, L. M.; Brown, T.; Norden, B. *Chem. Commun.* **2010**, *46*, 3714–3716.
- (42) Auyeung, E.; Macfarlane, R. J.; Choi, C. H. J.; Cutler, J. I.; Mirkin, C. A. *Adv. Mater.* **2012**, *24*, 5181–5186.
- (43) Datta, B.; Schuster, G. B.; McCook, A.; Harvey, S. C.; Zakrzewska, K. J. *Am. Chem. Soc.* **2006**, *128*, 14428–14429.
- (44) Datta, B.; Schuster, G. B. *J. Am. Chem. Soc.* **2008**, *130*, 2965–2973.
- (45) Chen, W.; Guler, G.; Kuruvilla, E.; Schuster, G. B.; Chiu, H. C.; Riedo, E. *Macromolecules* **2010**, *43*, 4032–4040.
- (46) Chen, W.; Schuster, G. B. *J. Am. Chem. Soc.* **2012**, *134*, 840–843.
- (47) Ma, Z. J.; Chen, W.; Schuster, G. B. *Chem. Mater.* **2012**, *24*, 3916–3922.
- (48) Chen, W.; Schuster, G. B. *J. Am. Chem. Soc.* **2013**, *135*, 4438–4449.
- (49) Chen, W.; Schuster, G. B. *Org. Biomol. Chem.* **2013**, *11*, 35–40.
- (50) Zhang, Z. L.; Wen, Y. Q.; Ma, Y.; Luo, J.; Jiang, L.; Song, Y. L. *Chem. Commun.* **2011**, *47*, 7407–7409.
- (51) Zhang, T.; Chen, P.; Sun, Y. W.; Xing, Y. Z.; Yang, Y.; Dong, Y. C.; Xu, L. J.; Yang, Z. Q.; Liu, D. S. *Chem. Commun.* **2011**, *47*, 5774–5776.
- (52) Slot, J. W.; Geuze, H. J. *Eur. J. Cell Biol.* **1985**, *38*, 87–93.
- (53) Grabar, K. C.; Freeman, R. G.; Hommer, M. B.; Natan, M. J. *Anal. Chem.* **1995**, *67*, 735–743.
- (54) Kuhlbrandt, W.; Downing, K. H. *J. Mol. Biol.* **1989**, *207*, 823–828.
- (55) Bredas, J. L.; Street, G. B. *Acc. Chem. Res.* **1985**, *18*, 309–315.
- (56) Zanchet, D.; Micheel, C. M.; Parak, W. J.; Gerion, D.; Alivisatos, A. P. *Nano Lett.* **2001**, *1*, 32–35.
- (57) Goodman, R. P.; Berry, R. M.; Turberfield, A. J. *Chem. Commun.* **2004**, 1372–1373.
- (58) Zheng, J. P.; Birktoft, J. J.; Chen, Y.; Wang, T.; Sha, R. J.; Constantinou, P. E.; Ginell, S. L.; Mao, C. D.; Seeman, N. C. *Nature* **2009**, *461*, 74–77.
- (59) Barrow, S. J.; Funston, A. M.; Wei, X. Z.; Mulvaney, P. *Nano Today* **2013**, *8*, 138–167.